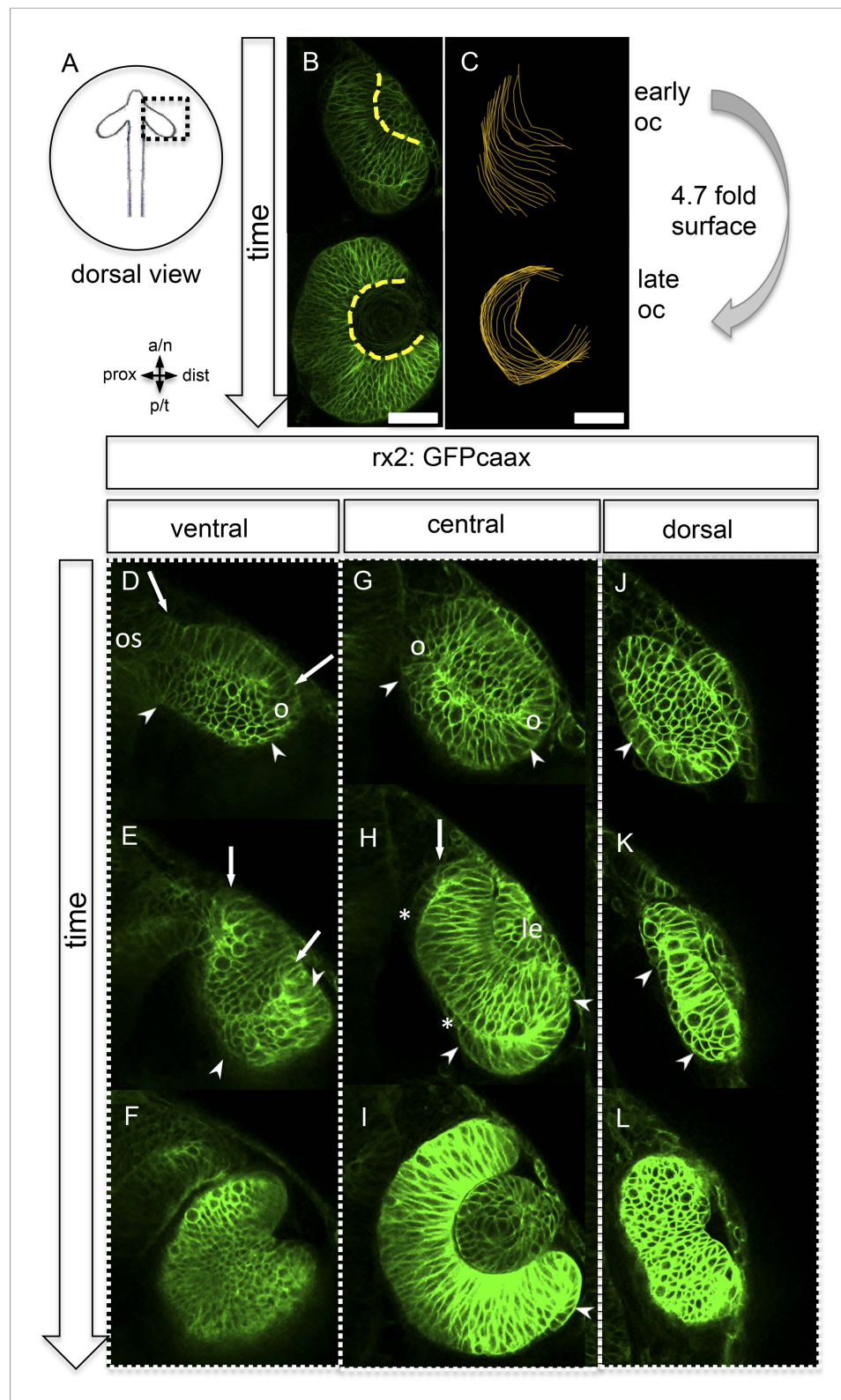


---

## Figures and figure supplements

Eye morphogenesis driven by epithelial flow into the optic cup facilitated by modulation of bone morphogenetic protein

**Stephan Heermann, et al.**



**Figure 1.** Neuroretinal surface increases during optic cup formation by epithelial flow. **(A)** Scheme showing the orientation of the pictures presented in **B–L**. **(B)** Basal neuroretinal surface increases from early to late optic cup stage (dashed yellow lines). **(C)** Basal neuroretinal surface was measured in 3D (superimposed orange lines), although RPCs undergo basal constriction during optic cup formation, the surface increases 4.7 fold from early to late optic cup stage. *Figure 1. continued on next page*

*Figure 1. Continued*

late optic cup stage, (**D–L**) transition from optic vesicle to optic cup over time, shown at a ventral (**D–F**), a central (**G–I**), and a dorsal (**J–L**) level. The membrane localized GFP is driven by an rx2 promoter (rx2::GFPcaax), which is active in RPCs. The optic vesicle is bi-layered (**D, G, J**) with a prospective lens-facing (arrows in **D** and **E**) and a prospective lens-averted (arrowheads in **D, G, J**) epithelium, connected to the forebrain by the optic stalk (os in **D**), at a ventral level both are connected at the distal site (circle in **D**), at a central level both are connected distally and proximally (circles in **G**), notably the morphology of the lens-averted epithelium at a dorsal level is different from central and ventral levels (arrowhead in **J**). Over time at ventral and central levels (**D–F** and **G–I**, respectively), the lens-averted epithelium is being integrated into the forming optic cup (arrowheads in **D, E, G, H, I** and arrow in **H**). A patch of cells in the lens-averted domain gives rise to the RPE (asterisks in **H** and arrowhead in **J, K**), le: developing lens, os: optic stalk, **B** and **D–L** were derived from 4D imaging data starting at 16.5 hpf (**D, G, J**), one focal plane is presented as **Video 1**, scalebar in **B** and **C** = 50  $\mu\text{m}$ .

DOI: [10.7554/eLife.05216.003](https://doi.org/10.7554/eLife.05216.003)

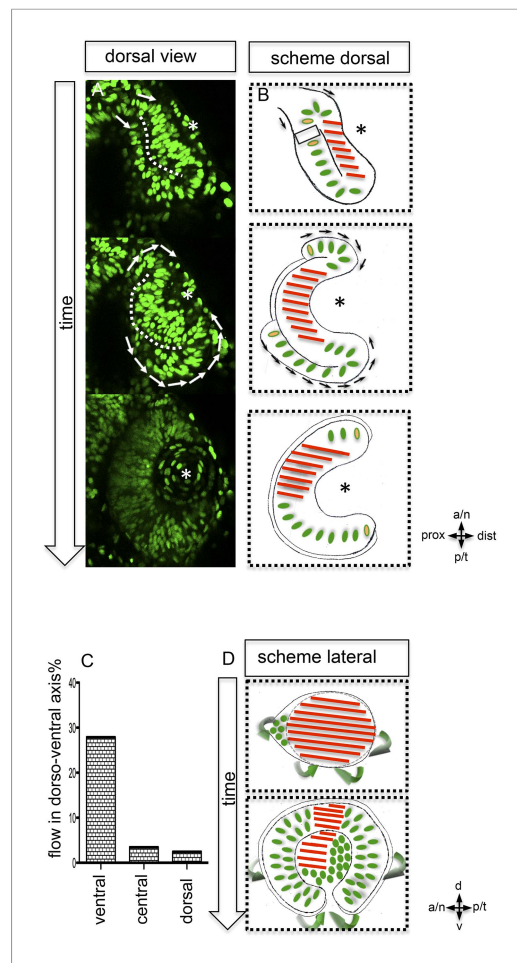


**Figure 2.** Neuroepithelial flow drives morphological changes from optic vesicle to optic cup: the role of the optic fissure and the impact on the forming stem cell domain. **(A)** Dorsal view on optic cup development over time visualized by mosaic nuclear GFP (H2BGFP) (data are derived from 4D imaging data started at 16.5 hpf (one optical section is provided as **Video 4**), while the lens-facing neuroepithelium is starting to engulf the developing lens (asterisk), the lens-verted epithelium is largely integrated into the lens-facing epithelium by flowing around the distal nasal and temporal rims (arrows). A white dotted line marks the border between lens-facing and lens-verted epithelium. **(B)** Scheme showing the key findings of **A**, the lens (asterisk) facing epithelium is marked with red bars. The lens-verted epithelium, which over time is integrated into the lens-facing epithelium is marked with green dots (except the cells at the edges are additionally marked with a yellow core). In between the last cells, which are integrated into the optic cup, the RPE will form in the lens-verted domain. **(C)** shows the percentage of movements with a considerable share in dorso-ventral direction for the dorsal, central, and ventral area of the developing eye. In the ventral area of the eye, there is significantly more movement in the dorso-ventral axis, than in the central or dorsal area. **(D)** scheme demonstrating the optic cup formation.

*Figure 2. continued on next page*

Figure 2. Continued

vesicle to optic cup transition (lateral view). Notably, the morphological change from the elongated oval optic vesicle to the hemispheric optic cup is driven mainly by the ventral regions (arrows mark the orientation of epithelial flow) (C and D).

DOI: 10.7554/eLife.05216.007

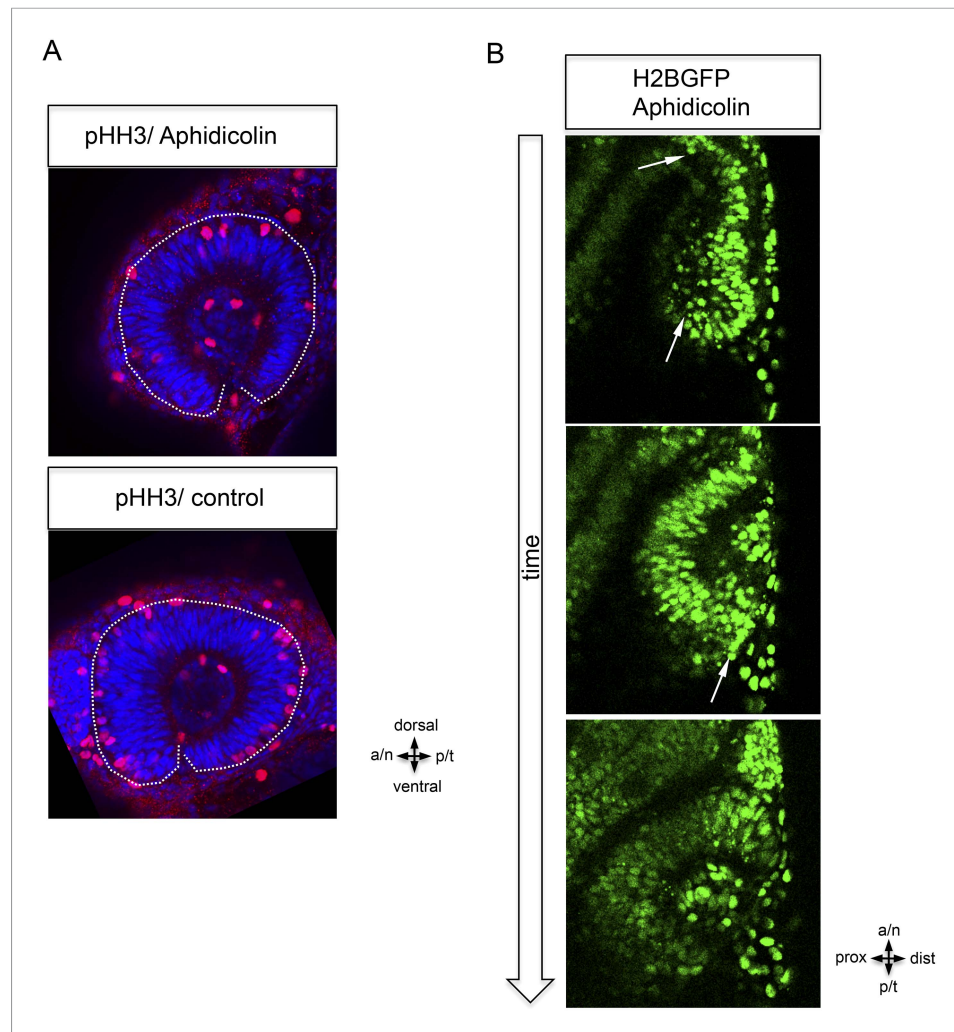


**Figure 2—figure supplement 1.** Epithelial flow is independent of cell division. (A) Retinal cell division was inhibited by application of aphidicolin, a well-established DNA polymerase inhibitor. Aphidicolin efficiently inhibited cell proliferation shown by drastically reduced pHH3 positive nuclei (upper panel, average of 6 pHH3 positive nuclei) compared to the control (lower panel, average of 21 pHH3 positive nuclei) (the optic cup is encircled with a dotted white line, 21.5 hpf). (B) We addressed the epithelial flow of aphidicolin-treated wild-type embryos, injected with H2BGFP RNA at the one cell stage; please see **Figure 2A** as control. The embryo was preincubated with aphidicolin 5 hr prior to the start of imaging (17 hpf, see also **Video 2**). The application of aphidicolin did not affect the epithelial flow. As a low level side effect of aphidicolin we observed cell death, in line with previous reports, importantly also not affecting the epithelial flow.

DOI: 10.7554/eLife.05216.008

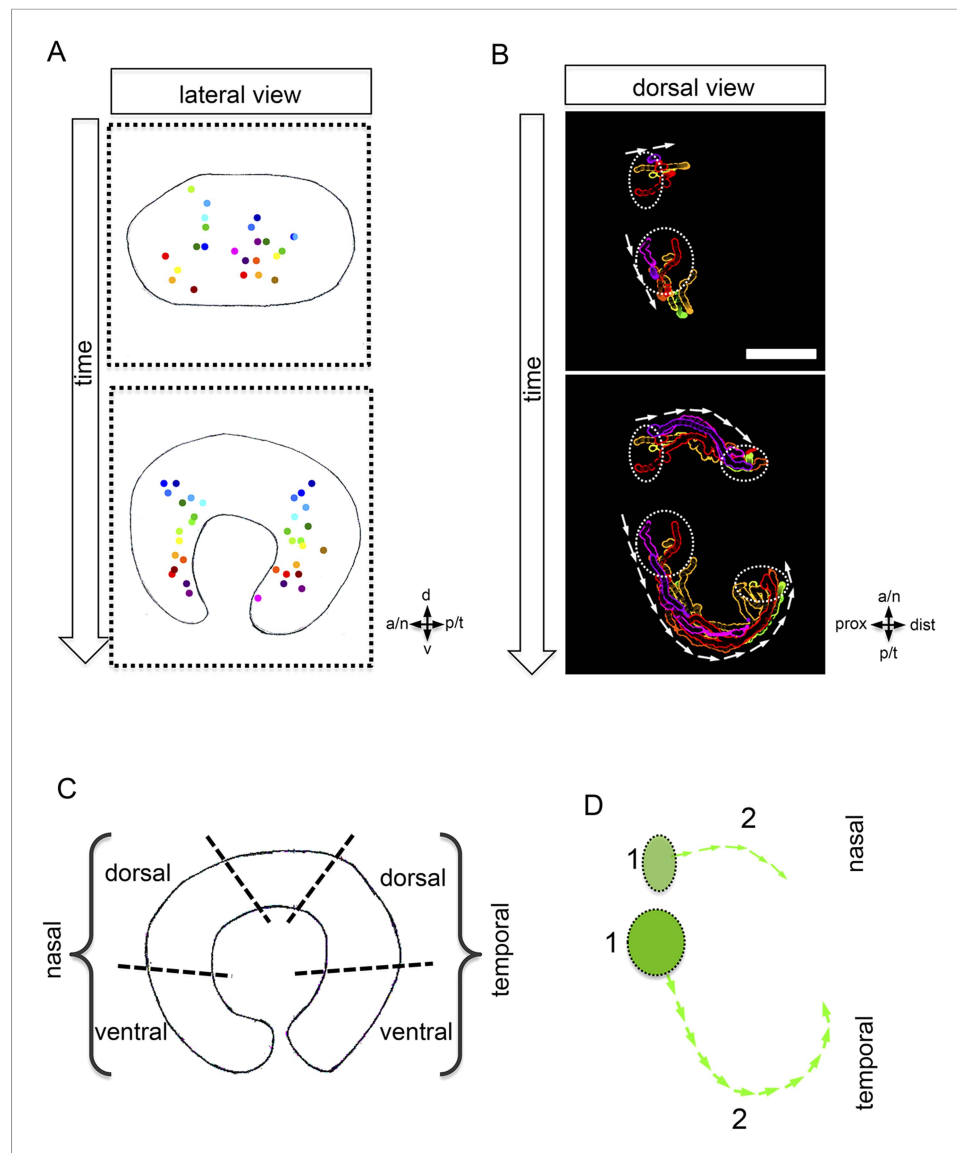


**Figure 3.** Development of the CMZ and quantification of the flow towards this domain. **(A)** scheme of optic cup development (lateral view over time) including the results of nuclear tracking from the presumptive CMZ back in time to the lens-averted epithelium, remarkably two distinct domains became apparent within the lens-averted epithelium as the source for the presumptive CMZ. **(B)** Establishment of the presumptive CMZ domain (dorsal view), nuclear tracking of cells (maximum projection) from the lens-averted domain (encircled in upper picture) eventually residing in the forming CMZ (additionally encircled in lower picture), scalebar = 50  $\mu\text{m}$ . **(C)** Scheme showing the optic cup from the lateral side. For quantification four domains were selected, nasal–dorsal, nasal–ventral, temporal–dorsal, and temporal–ventral. Note that the dorsal distal domain is only assembled secondarily and the ventral pole shows the optic fissure. **(D)** Based on differential effective distance, effective speed, and directionality, the migration distance was divided in two phases in the nasal and temporal domain, respectively.  
DOI: 10.7554/eLife.05216.009

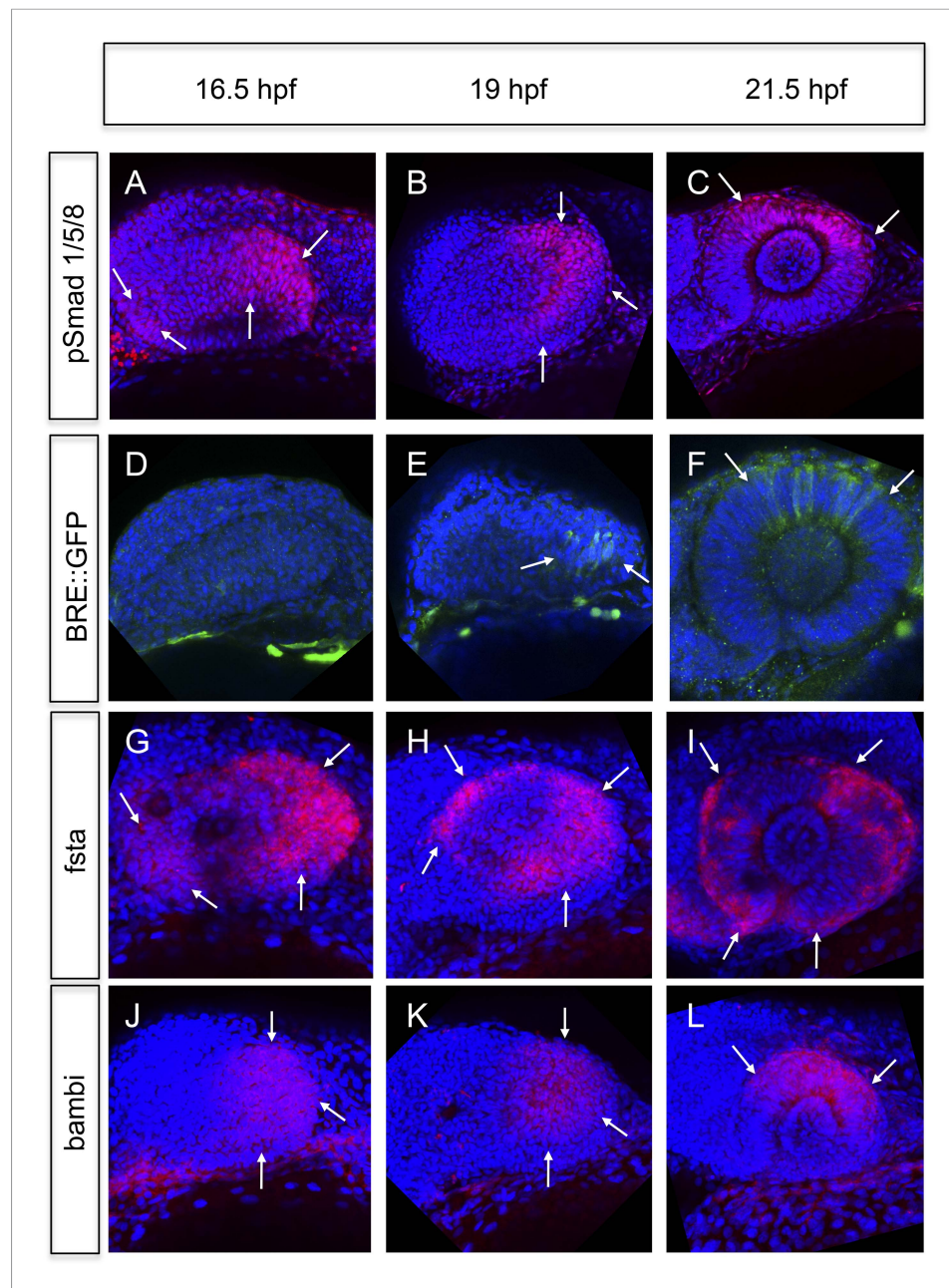


**Figure 4.** Analyses of BMP signaling and expression of BMP antagonists during development at 16.5 hpf, 19 hpf, and 21 hpf embryos are presented in a lateral view nasal left. (A–C) pSmad 1/5/8 immunohistochemistry (red) and DAPI nuclear staining. Activated BMP signaling can be appreciated mainly in the temporal domain of the optic vesicle (arrows) (A–B) and in the dorsal domain of the optic cup (arrows) (C). At 16.5 hpf, a small domain of activated BMP signaling is visible in the nasal optic vesicle (arrows) (A). (D–F) Immunohistochemically enhanced BRE::GFP (green) and DAPI nuclear staining. Activated BMP signaling can be appreciated in the temporal late optic vesicle (arrows) (E) and the dorsal optic cup (arrows) (F). Hardly any activity can be detected in the optic vesicle at 16.5 hpf. Note the delay of activity in comparison to pSmad 1/5/8. (G–I) Whole mount in situ hybridizations with a *fsta* probe (Fast Red) and DAPI nuclear staining. In the optic vesicle as well as in the optic cup two domains (nasal and temporal) of *fsta* expression can be seen (arrows). (J–L) Whole mount in situ hybridizations with a *bambi* probe (Fast Red) and DAPI nuclear staining. *Bambi* expression can be seen in the temporal domain of the optic vesicle (arrows) (J–K) and in the dorsal domain of the optic cup (arrows) (L).

DOI: [10.7554/eLife.05216.012](https://doi.org/10.7554/eLife.05216.012)

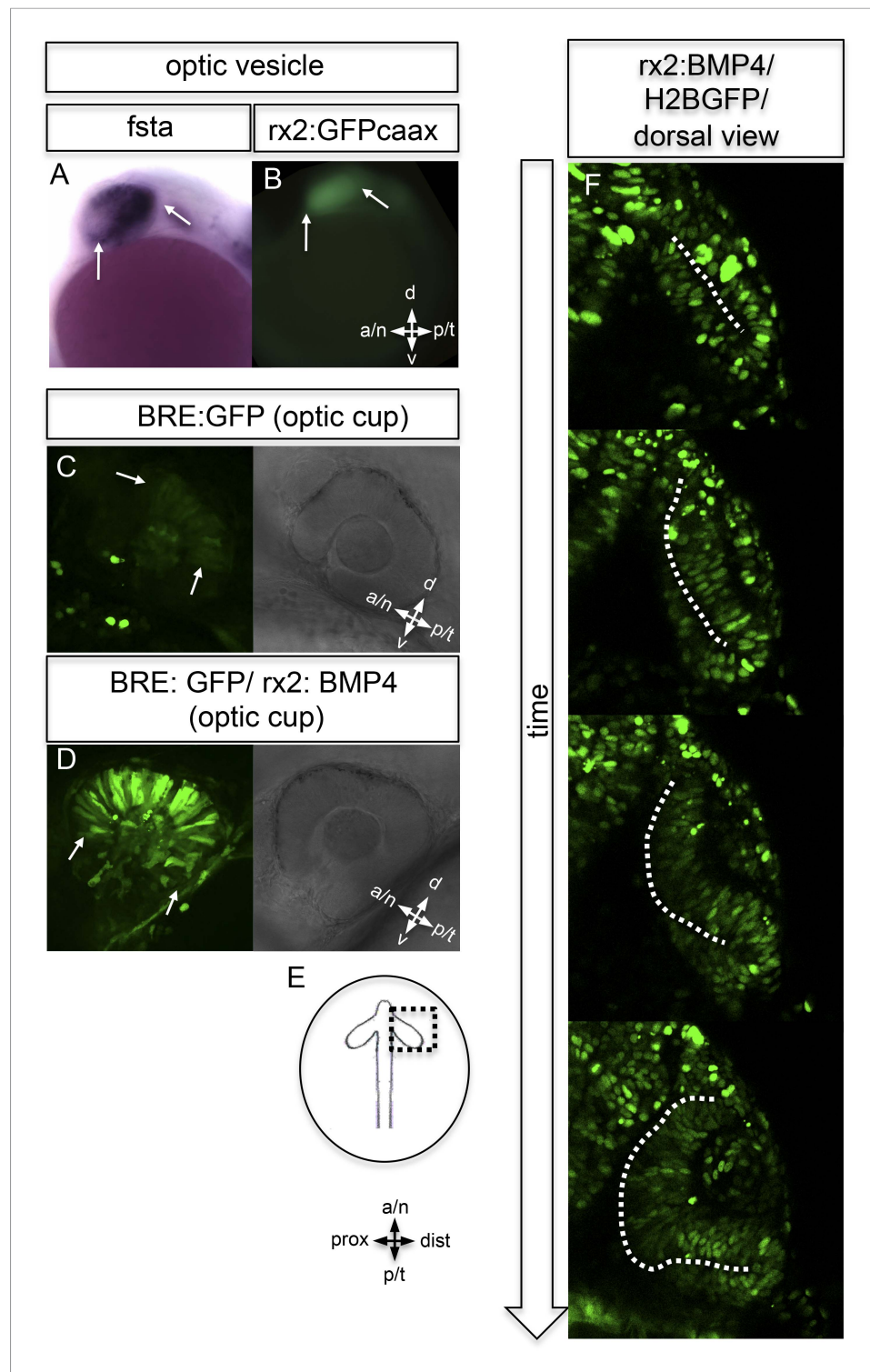


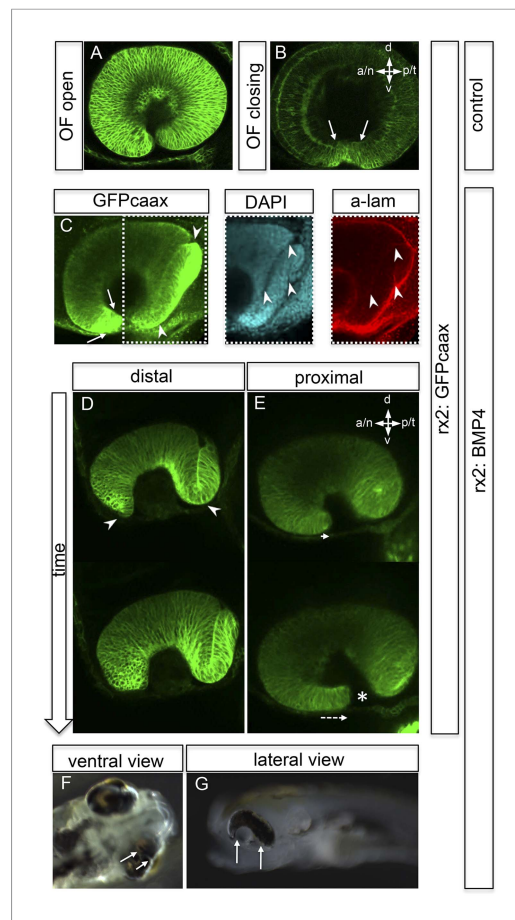
**Figure 5.** BMP antagonism drives neuroepithelial flow during optic cup formation. **(A)** whole mount in situ hybridization for *fsta* (NBT/BCIP) (17.5 hpf). **(B)** GFP expressed in the optic vesicle (arrows) of an *rx2::GFPcaax* zebrafish embryo (16.5 hpf), **(C–D)** GFP driven by the BRE and transmission/brightfield image for orientation. Strong GFP expression can be observed in the eye when BMP is driven under *rx2* (arrows in **D**), whereas only mild GFP can be observed in controls (arrows in **C**). **(E)** Scheme showing the orientation of the pictures presented in **F**, **(F)** optic cup development over time of an *rx2::BMP4* embryo. Cells are visualized by nuclear GFP (H2BGFP). A dotted line is indicating the border between lens-averted and lens-facing epithelium. Remarkably, the pan-ocular driven BMP

*Figure 5. continued on next page*

Figure 5. *Continued*

resulted in persisting lens-averted domains. The data presented in **F** are derived from 4D imaging data (start at 16.6 hpf) one optical section is also presented as **Video 6**.

DOI: [10.7554/eLife.05216.013](https://doi.org/10.7554/eLife.05216.013)



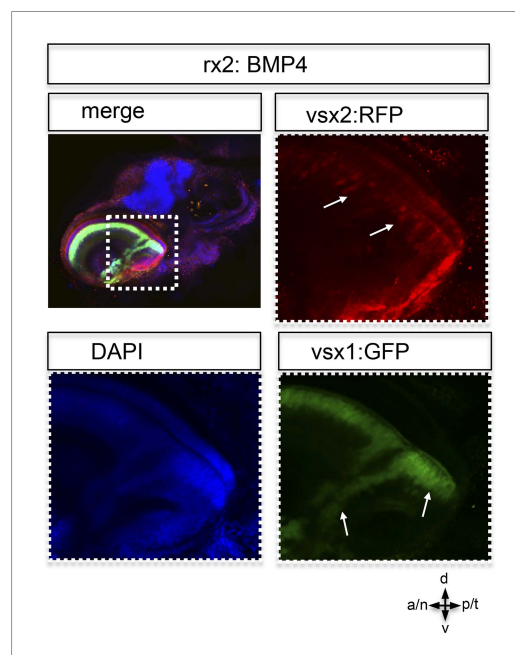
**Figure 6.** Impaired eye gastrulation results in coloboma. (A–B) Membrane-localized GFP (rx2::GFPcaax) in a developing eye during optic fissure closure (A = early, B = late) (lateral view, derived from imaging data, (A) start at 24 hpf, (B) after 34 hr imaging at 22°C). Rx2 is expressed in retinal stem cells/RPCs (A) and after NR differentiation is additionally expressed in photoreceptors and Müller Glia (B) while its expression is maintained in retinal stem cells of the CMZ (Reinhardt and Centanin et al., submitted). The optic fissure margins are still undifferentiated (arrows in B), (C) developing eye of rx2::BMP4 fish (lateral view), membrane-localized GFP (rx2::GFPcaax, anti-GFP immunointensified), DAPI nuclear labeling and anti-laminin immunostaining, the optic fissure is visible, noteworthy the temporal retina is misshaped and folded into the RPE domain (best visible in DAPI, arrowheads), and located on a basal membrane (arrowheads in anti-laminin), especially the temporal optic fissure margin (arrowheads in GFPcaax) is located in the folded part of the temporal retina and not facing the optic fissure (arrows in GFPcaax) (24 hpf) (D–E) impaired optic fissure closure in rx2::BMP4 embryos over time at a proximal (E) and a distal (D) level. (Data obtained from 4D imaging of rx2::BMP4/ rx2::GFPcaax started at 21.5 hr. Data are also presented as **Video 10**.) Importantly, next to the affected temporal optic cup also the nasal optic cup is mis-folded (arrowheads in D). *Figure 6. continued on next page*

Figure 6. Continued

Figure 6. continued on next page

Remarkably, however, the nasal optic fissure margin extends into the optic fissure (dashed arrow in **E**) but the temporal optic fissure margin does not, likely being the result of the intense mis-bending of the temporal optic cup. This results in a remaining optic fissure (asterisk in **E**). (**F–G**) Brightfield images of variable phenotype intensities observed in *rx2::BMP4* hatchlings.

DOI: [10.7554/eLife.05216.016](https://doi.org/10.7554/eLife.05216.016)



**Figure 6—figure supplement 1.** Postembryonic eye development of *rx2::BMP4* hatchlings. Although the temporal optic cup is largely malformed and folded it can be seen clearly, that *vsx1* as well as *vsx2* transgenes (intensified by wholemount immunohistochemistry) are expressed in the folded epithelium (arrows). This indicates at least a partial correct differentiation into neuroretinal tissue.

DOI: [10.7554/eLife.05216.017](https://doi.org/10.7554/eLife.05216.017)

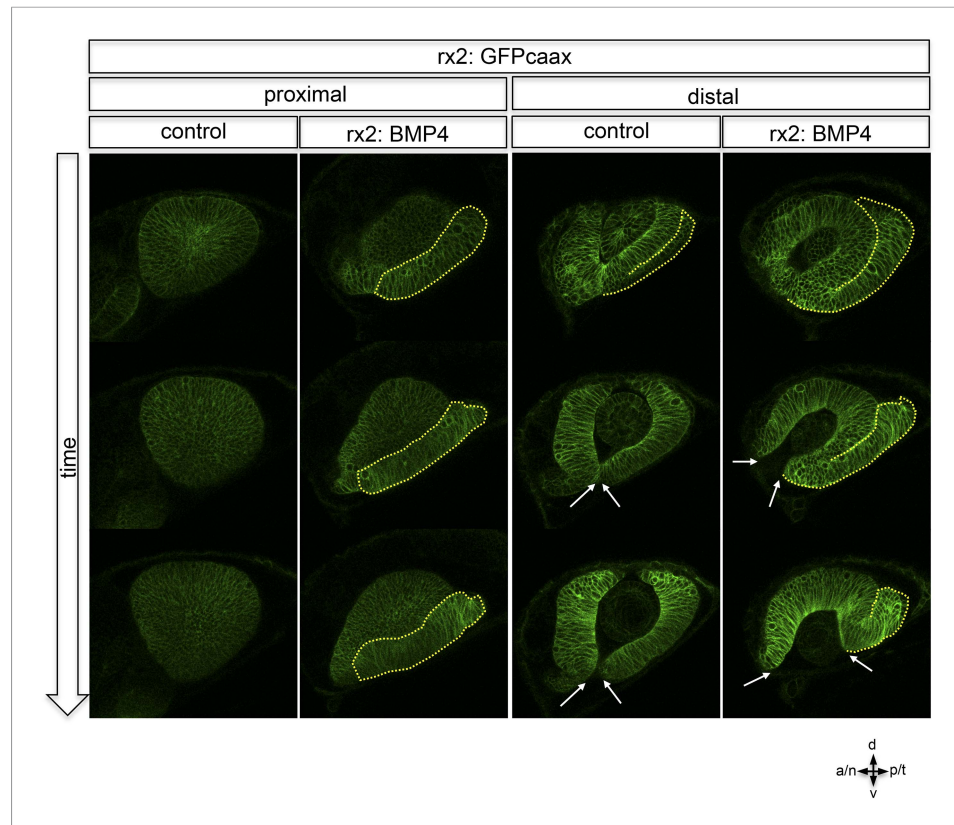


**Figure 6—figure supplement 2.** Lateral view on optic cup development over time, rx2::GFPcaax (control) is compared to rx2::BMP4 at proximal and distal levels. While in controls the lens-averted domain (yellow dotted line) is integrated into the developing optic cup it persists in rx2::BMP4 embryos. Note the increasing optic fissure (arrows) in rx2::BMP4 embryos. These data were obtained by 4D imaging (start at 20 hpf) and are also presented as **Video 8** and **Video 9**.

DOI: [10.7554/eLife.05216.018](https://doi.org/10.7554/eLife.05216.018)

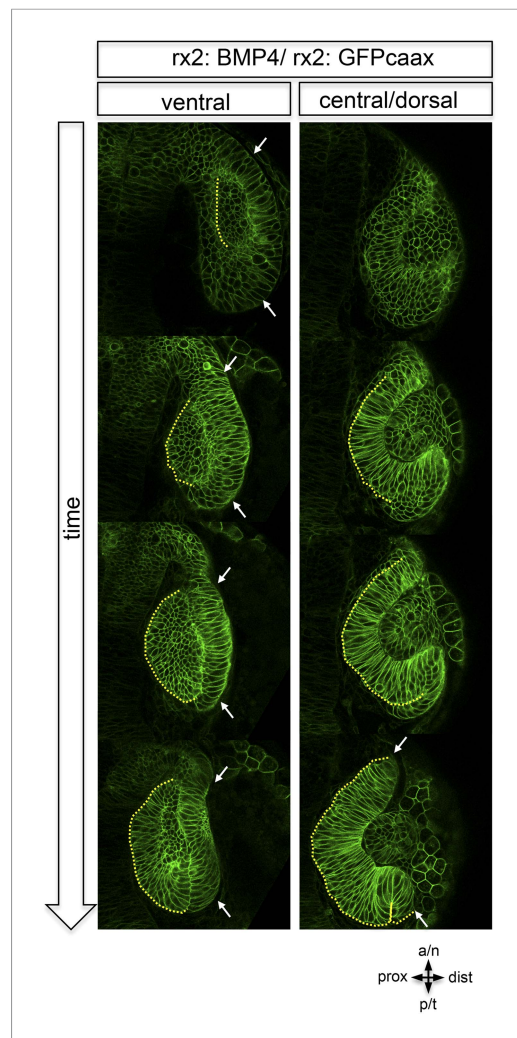


**Figure 6—figure supplement 3.** Dorsal view on optic cup development of an *rx2::BMP4* embryo over time at ventral vs central/ dorsal levels. The yellow dotted line indicates the border between the lens-facing and the lens-averted domain. Remarkably, the lens-averted domain is not integrated into the optic cup (compare to **Figures 1 and 2**). Notably, an altered morphology of the ventral optic vesicle can be observed showing the domain which is not going to be integrated (arrows). These data are derived from imaging data (start at 19 hpf) which is presented in **Video 7**.

DOI: [10.7554/eLife.05216.019](https://doi.org/10.7554/eLife.05216.019)

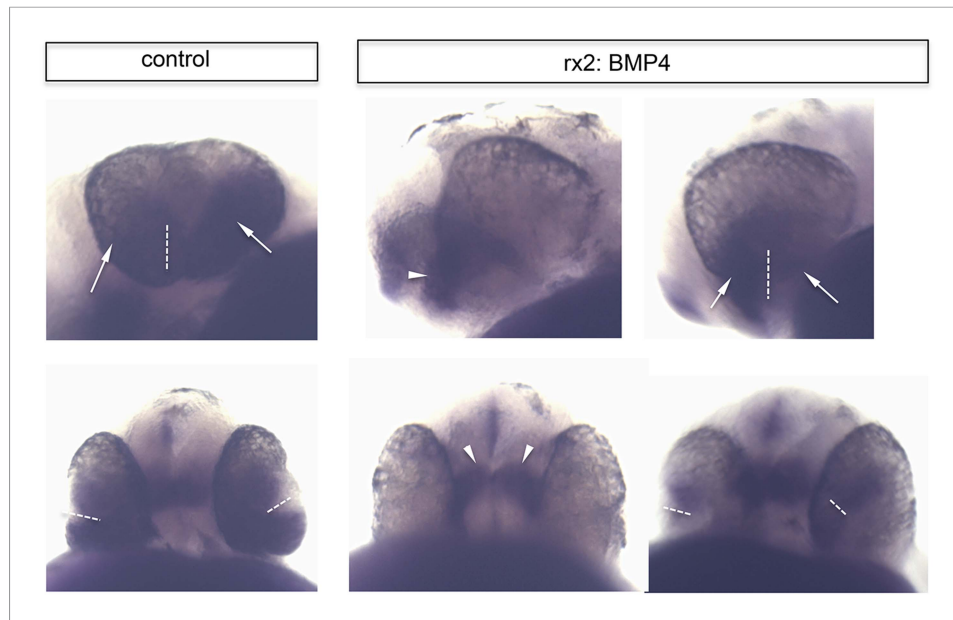


**Figure 6—figure supplement 4.** Ventral retinal identity remains in rx2::BMP4 embryos. Whole mount in situ hybridization with a *vax2* probe (NBT/BCIP) of control (left) and rx2::BMP4 embryos (right) in a lateral view (upper pictures) and a ventral view (lower pictures) (28 hpf). Note that the ventral retinal marker remains expressed in the forming ventral optic cup even if BMP4 is expressed panocularly (rx2::BMP4). Also note that the *vax2* domain in control is broader than in the rx2::BMP4 embryos (arrows) in which it is more prominent in the optic stalk region (arrowhead) (the dotted line indicates the optic fissure).

DOI: [10.7554/eLife.05216.020](https://doi.org/10.7554/eLife.05216.020)